*Inorg. Chem.* **2003**, *42*, 960–969

# Water Displacement by Cyanogold Complexes in Binuclear Nickel(II) Compounds Based on Bridging Oxalate. Synthesis, Structural Diversity, Magnetic Properties, and DFT Calculations

**Pablo Vitoria,[†] Iñaki Muga,[†] Juan M. Gutiérrez-Zorrilla,*[,†] Antonio Luque,[†] Pascual Román,[†] Luis Lezama,[†] F. Javier Zúniga,[‡] and Javier I. Beitia[§]**

*Departamento de Química Inorgánica and Departamento de Física de la Materia Condensada, Facultad de Ciencias, Universidad del País Vasco, Apartado 644, E-48080 Bilbao, Spain*

Received May 7, 2002

Several cyanogold complexes react with the binuclear nickel complex $[\{Ni(dien)(H_2O)\}_2(\mu\text{-ox})](PF_6)_2 \cdot 2H_2O$ to give the compounds $[\{Ni(dien)(H_2O)\}_2(\mu\text{-ox})]Br_2$ (**1**), $[\{Ni(dien)(Au(CN)_2)\}_2(\mu\text{-ox})]$ (**2**), and $[\{Ni(dien)\}_2(\mu\text{-ox})\{\mu\text{-Au}(CN)_4\}](PF_6)$ (**3**) (dien, diethilenetriamine; ox, oxalate). In the case of compounds **2** and **3**, water displacement by the corresponding cyanogold complex takes place, whereas compound **1** is formed by a substitution of the anion. The crystal structures of compounds **1** and **2** present a 2D arrangement where the layers are connected by van der Waals forces (**1**) or N–H···N≡C hydrogen bonds (**2**), where each binuclear complex is hydrogen bonded to its neighbors, whereas compound **3** presents a novel structure where the tetracyanoaurate acts as a bridging ligand to give a polymeric compound. Magnetic studies of these compounds reveal an antiferromagnetic behavior. Finally, density functional theory (DFT) calculations have been performed on isolated models of compounds **2** and **3** in order to gain some insight about the different behavior of the $[Au(CN)_2]^-$ and $[Au(CN)_4]^-$ groups as ligands and proton acceptors in hydrogen bonds.

## Introduction

The design and synthesis of molecular magnetic materials has been the focus of increasing attention over the past 3 decades.[1] The study of magnetic interactions in di- and polynuclear complexes as a function of structural and electronic factors (coordination polyhedron, donor atoms, nature of substituents of the peripheral ligands, and orbital topology) is still a main challenge in inorganic chemistry. Significant research has been devoted to analyzing the oxalate group to act as a bridging ligand from both experimental[2] and theoretical[3] viewpoints. Polymeric compounds containing the "building block" $[\{M(L)\}_2(\mu\text{-ox})]^{n+}$ connected through anionic ligands, other than oxalate, such as perchlorate,[4] hydrogenphosphate,[5] chloride,[6] and azide[7] have been described.

The controlled assembly of inorganic blocks is very important in the design of high-dimensionality systems. An approach to the synthesis of these materials is to use $[M(CN)_n]^{y-}$ groups in conjunction with a transition metal ion complex, due to the ability of the cyano group to connect various central atoms for building molecular assemblies with various degrees of dimensionality.[8] The use of cyano

* Author to whom correspondence should be addressed. E-mail: qipguloj@lg.ehu.es.

[†] Departamento de Química Inorgánica

[‡] Departamento de Física de la Materia Condensada

[§] Current address: Departamento de Química Inorgánica, Facultad de Farmacia, Apartado 450, 01080 Vitoria, Spain.

(1) (a) Gatteschi, D.; Khan, O.; Miller, J. S.; Palacio, F. *Magnetic Molecular Materials*; Kluwer: Dordrecht, The Netherlands, 1991. (b) Bruce, Q. W., O'Hare D., Eds. *Inorganic Materials*; Wiley: Chichester, U.K., 1992. (c) Khan, O. *Molecular Magnetism*; VCH: New York, 1993. (d) Decurtins, S.; Schmalle, H. W.; Pellaux, R.; Fischer, P.; Hauser, A. *Mol. Cryst. Liq. Cryst.* **1997**, *305*, 227.

(2) (a) Kahn, O. *Angew. Chem., Int. Ed. Engl.* **1985**, *24*, 834. (b) Julve, M.; Verdaguer, M.; Kahn, O.; Gleizes, A.; Philoche-Levisalles, O. *Inorg. Chem.* **1983**, *22*, 368. (c) Julve, M.; Verdaguer, M.; Kahn, O.; Gleizes, A.; Philoche-Levisalles, O. *Inorg. Chem.* **1984**, *23*, 3808. (d) Glerup, J.; Goodson, P. A.; Hodgson, D. J.; Michelsen, K. *Inorg. Chem.* **1995**, *34*, 6255.

(3) (a) Cabrero, J.; Ben Amor, N.; de Graaf, C.; Illas, F.; Caballol, R. *J. Phys. Chem. A* **2000**, *104*, 9983. (b) Alvarez, S.; Julve, M.; Verdaguer, M. *Inorg. Chem.* **1990**, *29*, 4500. (c) Cano, J.; Alemany, P.; Alvarez, S.; Verdaguer, M.; Ruiz, E. *Chem. Eur. J.* **1998**, *4*, 476. (d) Escuer, A.; Vicente, R.; Ribas, J.; Jaud, J.; Raynaud, B. *Inorg. Chim. Acta* **1994**, *216*, 139. (e) Escuer, A.; Vicente, R.; El Fallah, M. S.; Jaud, J. *Inorg. Chim. Acta* **1995**, *232*, 151. (f) Román, P.; Guzmán-Miralles, C.; Luque, A.; Beitia, J. I.; Cano, J.; Lloret, F.; Julve, M.; Alvarez, S. *Inorg. Chem.* **1996**, *35*, 3741.

(4) Min, K. S.; Suh, M. P. *J. Solid State Chem.* **2000**, *152*, 183

(5) Choudhury, A.; Natarajan, S.; Rao C. N. R. *Chem.-Eur. J.* **2000**, *6*, 1168.

(6) Decurtins, S.; Schmalle, H. W.; Schneuwly, P.; Zheng, L.-M.;. Ensling, J.; Hauser, A. *Inorg. Chem.* **1995**, *34*, 5501.

(7) Escuer, A.; Vicente, R.; Solans, X.; Font-Bardia, M. *Inorg. Chem.* **1994**, *33*, 6007.



10.1021/ic0203217 CCC: $25.00 
Published on Web 01/17/2003

**Scheme 1**

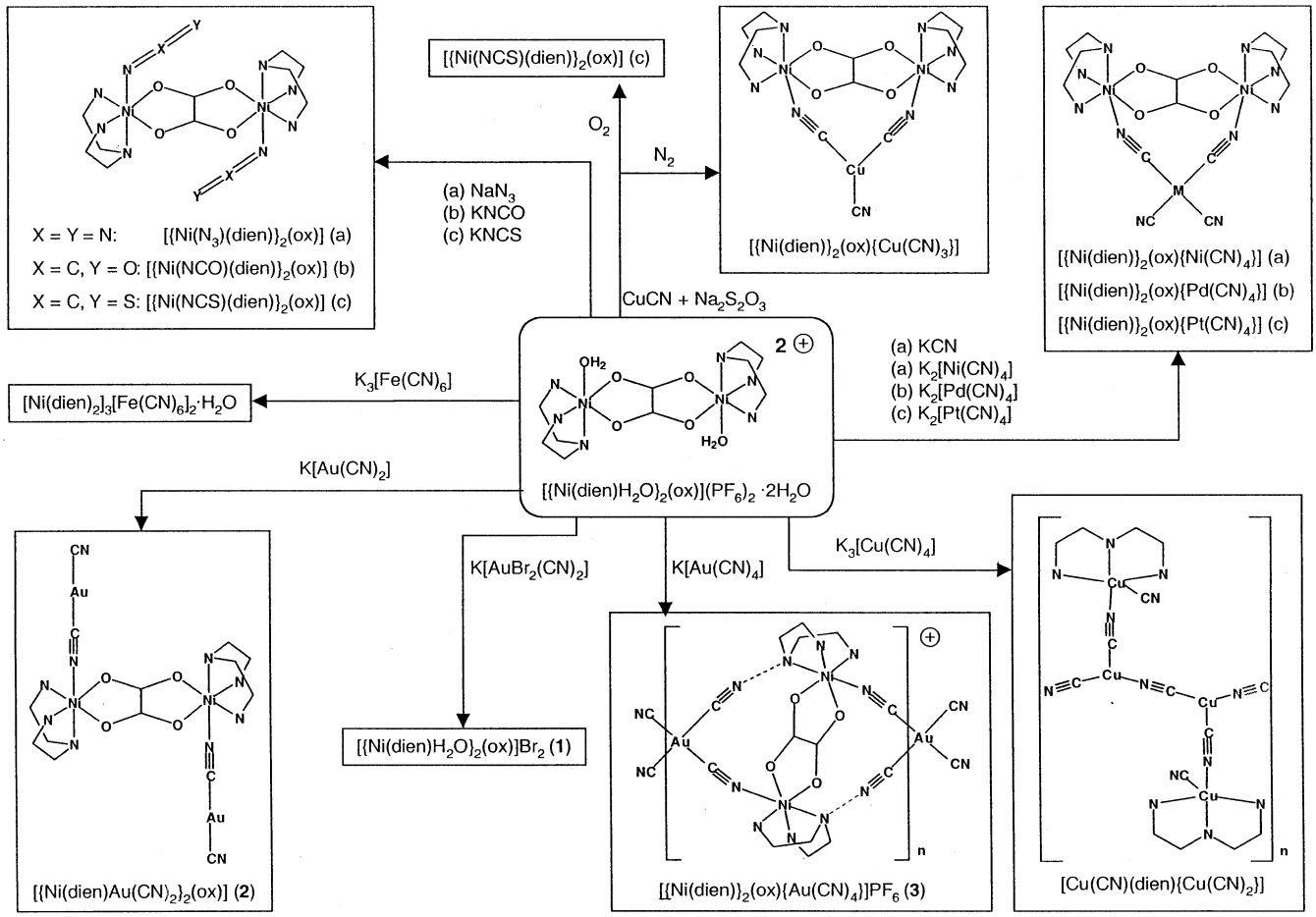


complexes as precursors for homo- and heterobimetallic catalysts[9] and photosensitizers[10] has also been reported. Since the cyanide linkages permit an interaction between paramagnetic centers, cyanometalate building blocks have found useful applications in the field of molecular magnets.[11]

This work forms a part of our research program on the chemistry of first-row transition metal oxalate complexes,[12] which intends to analyze the effect of the peripheral ligands on the structural diversity and magnetic properties of oxalate bridged compounds. We have employed the nickel binuclear compound $[\{Ni(dien)(H_2O)\}_2(\mu\text{-ox})](PF_6)_2 \cdot 2H_2O$ due to the lability of its water molecules, which may be replaced by a plethora of ligands, such as the pseudohalide ligands ($N_3^-$, $NCO^-$, $NCS^-$) and, due to the attractiveness of polymers comprised of M−CN−M′ units, $CN^-$ and the cyano complexes $[M(CN)_n]^{y-}$ (M: Ni, Pd, Pt, Cu, Ag, and Au (Scheme 1)). In this paper we report the synthesis, crystal structure,

(8) (a) Cernak, J.; Orendac, M.; Potocnak, I.; Chomic, J.; Orendacova, A.; Skorsepa, J.; Feher, A. *Coord. Chem. Rev.* **2002**, *224*, 51. (b) Ohba, M.; Maruono, N.; Okawa, H.; Enoki T.; Latour, J. *J. Am. Chem. Soc.* **1994**, *116*, 11566. (c) Entley W. R.; Girolami, G. S. *Science* **1995**, *268*, 397. (d) Sato, O.; Iyoda, T.; Fujishima A.; Hashimoto, K. *Science* **1996**, *271*, 49. (e) Miyasaka, H.; Matsumoto, N.; Okawa, H.; Re, N.; Gallo E.; Floriani, C. *J. Am. Chem. Soc.* **1996**, *118*, 981. (f) Mallah, T.; Thiebaut, S.; Verdaguer, M.; Veillet, P. *Science* **1993**, *262*, 1554. (g) Vahrenkamp, H.; Geiss A.; Richardson, G. N. *J. Chem. Soc., Dalton Trans.* **1997**, 3643.

(9) (a) Funabiki, T.; Yoshida, S.; Tarama, K. *J. Chem. Soc., Chem. Commun.* **1978**, 1059. (b) Fujita, M.; Kwon, Y. J.; Washizu, S.; Ogura, K. *J. Am. Chem. Soc.* **1994**, *116*, 1151. (c) Brahmi, R.; Kappenstein, C.; Cernak, J.; Duprez, D. Sadel, A. Stud. *J. Chim. Phys. Phys.-Chim. Biol.* **1999**, *96*, 487. (d) Rosas, N.; Cabrera, A.; Sharma, P.; Arias, J. L.; García, J. L. Arzoumanian, H. *J. Mol. Catal. A: Chem.* **2000**, *156*, 103.

(10) (a) Heimer, T. A.; Bignozzi, C. A.; Meyer, G. J. *J. Phys. Chem.* **1993**, *97*, 11987. (b) Goncalves, I. S.; Kuhn, F. E.; Lopes, A. D.; Parola, A. J.; Pina, F.; Sotomayor, J.; Romao, C. C. *J. Organomet. Chem.* **1998**, *560*, 117. (c) Ferrere, S. *Chem. Mater.* **2000**, *12*, 1083.

(11) (a) Pilkington, M.; Decurtins, S. *Chimia* **2000**, *54*, 593. (b) Weihe, H.; Gaudel, H. U. *Comments Inorg. Chem.* **2000**, *22*, 75. (c) Ohba, M.; Okawa, H. *Coord. Chem. Rev.* **2000**, *198*, 313. (d) Verdaguer, M.; Bleuze, A.; Marvaud, V.; Vaissermann, J.; Seuleiman, M.; Deplanches, C.; Scuiller, A.; Train, C.; Garde, R.; Gelly, G.; Lomenech, C.; Rosenman, I.; Veillet, P.; Cartier, C.; Villain, F. *Coord. Chem. Rev.* **1999**, *190*−*192*, 1023. (e) Ouahab, L. *Coord. Chem. Rev.* **1998**, *178*−*180*, 1501. (f) Clemente-Leon, M.; Coronado, E.; Galan-Mascaros, J. R.; Gomez-Garcia, C. J.; Woike, Th.; Clemente-Juan, J. M. *Inorg. Chem.* **2001**, *40*, 87. (g) Marvilliers, A.; Mallah, T.; Riviere, E.; Parsons, S.; Munoz, C.; Vostrikova, K. E. *Mol. Cryst. Liq. Cryst. Sci. Technol., Sect. A* **1999**, *335*, 1195. (h) Colacio, E.; Ghazi, M.; Stoeckli-Evans, H.; Lloret, F.; Moreno, J. M.; Perez, C. *Inorg. Chem.* **2001**, *40*, 4876.

(12) (a) Muga, I.; Gutiérrez-Zorrilla, J. M.; Luque, A.; Román, P.; Lloret, F. *Inorg. Chem.* **1997**, *36*, 743. (b) Castillo, O.; Muga, I.; Luque, A.; Gutiérrez-Zorrilla, J. M.; Sertucha, J.; Vitoria, P.; Román, P. *Polyhedron* **1999**, *18*, 1235. (c) Muga, I.; Gutiérrez-Zorrilla, J. M.; Vitoria, P.; Luque, A.; Insausti, M.; Román, P.; Lloret, F. *Eur. J. Inorg. Chem.* **2000**, *12*, 2541. (d) Castillo, O.; Luque, A.; Lloret, F.; Román, P. *Inorg. Chim. Acta* **2001**, *324*, 141. (e) Castillo, O.; Luque, A.; Roman, P.; Lloret, F.; Julve, M. *Inorg. Chem.* **2001**, *40*, 5526. (f) Guzmán-Miralles, C.; Castillo, O.; Luque, A.; Beitia, J. I.; Román, P. *Acta Crystallogr.* **2001**, *E57*, m407. (g) Muga, I.; Vitoria, P.; Gutiérrez-Zorrilla, J. M.; Luque, A.; Guzmán-Miralles, C.; Román, P. *Acta Crystallogr.* **2002**, *C58*, m81.

magnetic properties, and density functional theory (DFT) calculations for the compounds $[\{Ni(dien)(H_2O)\}_2(\mu\text{-ox})]Br_2$ (**1**), $[\{Ni(dien)\{Au(CN)_2\}\}_2(\mu\text{-ox})]$ (**2**), and $[\{Ni(dien)\}_2(\mu\text{-ox})\{\mu\text{-}Au(CN)_4\}](PF_6)$ (**3**), obtained from the above-mentioned precursor and the cyanogold complexes $K[AuBr_2(CN)_2]$, $K[Au(CN)_2]$, and $K[Au(CN)_4]$, respectively. Compound **1** belongs to a series of 2D isomorphic compounds in which the interlamellar distance correlates with the counteranion dimensions. Three compounds with the $[Au(CN)_2]^-$ unit as ligand have been described.[13] Compound **3** is the first example in which the tetracyanoaurate acts as a bridging ligand to give a polymeric compound.

## Experimental Section

**Materials.** Bromine ($Br_2$, Fluka), gold shot (Au, Aldrich), potassium cyanide (KCN, Fluka), silver hexafluorophosphate ($AgPF_6$, Strem), and methanol ($CH_3OH$, Merck) were used as commercially received. The binuclear nickel complex, $[\{Ni(dien)(H_2O)\}_2(\mu\text{-ox})]Cl_2$[3f] and the gold complexes, $K[AuBr_2(CN)_2]$[14] and $K[Au(CN)_4]$,[15] were prepared according to literature methods. The complex $[\{Ni(dien)(H_2O)\}_2(\mu\text{-ox})](PF_6)_2\cdot 2H_2O$ was obtained by addition of silver hexafluorophosphate to an aqueous solution of $[\{Ni(dien)(H_2O)\}_2(\mu\text{-ox})]Cl_2$. Potassium dicyanoaurate(I), $K[Au(CN)_2]$, was prepared by bubbling atmospheric oxygen in an aqueous solution containing potassium cyanide and gold in shots until gold was completely dissolved.

**Synthesis of Complexes. (a) $[\{Ni(dien)(H_2O)\}_2(\mu\text{-ox})]Br_2$ (1).** An aqueous solution (30 mL) of $K[AuBr_2(CN)_2]$ (0.45 g, 1.00 mmol) was added under stirring to a solution of 0.52 g (0.67 mmol) of $[\{Ni(dien)(H_2O)\}_2(\mu\text{-ox})](PF_6)_2\cdot 2H_2O$ in water. After several days of slow evaporation at room temperature, blue prismatic crystals of the compound were obtained. Anal. Calcd for $C_{10}H_{30}Br_2N_6Ni_2O_6$ (**1**): C, 19.77; H, 4.98; N, 13.83%. Found: C, 19.08; H, 4.81; N, 13.84%. Main IR features ($cm^{-1}$): oxalate ligand, 1635 vs, 1355 s, 1315 s, 805 m.

**(b) $[\{Ni(dien)(Au(CN)_2)\}_2(\mu\text{-ox})]$ (2).** A solution of 0.15 g (0.52 mmol) of $K[Au(CN)_2]$ in 50 mL of water was added dropwise to an aqueous solution (50 mL) of $[\{Ni(dien)(H_2O)\}_2(\mu\text{-ox})](PF_6)_2\cdot 2H_2O$ (0.21 g, 0.27 mmol). The resulting blue solution was filtered on a grade 3 glass sinter. After a week, blue spherulites of the compound appeared upon slow evaporation of the solvent at room temperature. To obtain X-ray suitable crystals, a $K[Au(CN)_2]$ methanolic solution was layered over an aqueous solution of the precursor hexafluorophosphate salt. Anal. Calcd for $C_{14}H_{26}Au_2N_{10}Ni_2O_4$ (**2**): C, 18.48; H, 2.88; N, 15.40%. Found: C, 17.66; H, 2.66; N, 15.31%. Main IR features ($cm^{-1}$): cyanide ligand, 2185 w, 2155 s; oxalate ligand, 1635 vs, 1360 m, 1315 s, 795 s.

**(c) $[\{Ni(dien)\}_2(\mu\text{-ox})\{\mu\text{-}Au(CN)_4\}][PF_6]$ (3).** A solution of 0.04 g (0.12 mmol) of $K[Au(CN)_4]$ in 10 mL of water was added dropwise to an aqueous solution (50 mL) of $[\{Ni(dien)(H_2O)\}_2(\mu\text{-ox})][PF_6]_2\cdot 2H_2O$ (0.10 g, 0.12 mmol). The resulting blue solution was filtered and allowed to stand for 6 days. Blue square crystals were obtained. Anal. Calcd for $C_{14}H_{26}AuF_6N_{10}Ni_2O_4P$ (**3**): C, 19.60; H, 3.06; N, 16.33%. Found: C, 18.87; H, 2.89; N, 16.11%. Main IR features ($cm^{-1}$): cyanide ligand, 2220 vw, 2188 vw; oxalate ligand, 1650 vs, 1355 m, 1315 s, 795 s; hexafluorophosphate anion, 850 vs.

**Physical Techniques.** Carbon, nitrogen, and hydrogen were determined by organic microanalysis on a LECO CHNS 932 analyzer. Infrared spectra were obtained (KBr pellets) on a Mattson 1000 FT-IR spectrometer. Magnetic susceptibility measurements were performed on powdered samples with a Quantum Design MPMS-7 Squid magnetometer. The magnetic field used in the experiments was of 0.1 T, a value at which the magnetization versus magnetic field curve was still linear at 1.8 K. Experimental susceptibility values were corrected for the diamagnetic contributions and for the temperature-independent paramagnetism.

**X-ray Data Collection and Structure Determination.** Room-temperature single-crystal collections for **1** − **3** were performed with an Enraf-Nonius CAD-4 four circle diffractometer using graphite monochromatized Mo Kα radiation ($\lambda = 0.710\ 69$ Å) and operating in the $\omega-2\theta$ scan mode. Platelike single crystals of **1**−**3** of dimensions $0.75 \times 0.25 \times 0.10$, $0.45 \times 0.45 \times 0.07$, and $0.44 \times 0.4 \times 0.10$ mm, respectively, were used for data collection. The unit cell parameters were calculated by least-squares fit of well-centered reflections in the ranges $6 < \theta < 15$ (**1**), $10 < \theta < 22$ (**2**), and $9 < \theta < 15$ (**3**). Intensities of two reflections monitored periodically exhibited no significant variation. Data were corrected for Lorentz and polarization effects. An empirical absorption correction following the procedure DIFABS[16] was applied to data for compounds **1** and **3**, resulting in transmission factors ranging from 0.215 to 0.578 for **1** and from 0.093 to 0.510 for **3**. For compound **2**, the indices and distances of the faces of the crystal were measured, and an analytical absorption correction was applied, resulting in transmission factors ranging from 0.023 to 0.406. Neutral atom scattering factors and anomalous dispersion factors were taken from the literature.[17] Experimental details and crystal data for the three compounds are given in Table 1.

The structures were solved using Patterson methods[18] (DIRDIF99) and refined by full-matrix least-squares analysis using the SHELXL-97 program.[19] All non-hydrogen atoms were refined anisotropically. Hydrogen atoms of the water molecule in compound **1** and of the central nitrogen atom of the dien ligand in all compounds were located in the difference Fourier map and refined isotropically. All the other H atoms were placed in calculated positions and refined using the riding model. The calculations were carried out using WINGX[20] running on a personal computer.

**Computational Details.** Calculations have been performed for the cyano complexes $[Au(CN)_2]^-$ (linear) and $[Au(CN)_4]^-$ ($D_{4h}$ symmetry) and for the isolated molecular dimers $[\{Ni(dien)(H_2O)\}_2(\mu\text{-ox})]^{2+}$ (Figure 1, excluding bromides), $[\{Ni(dien)\{Au(CN)_2\}\}_2(\mu\text{-ox})]$ (Figure 2), and $[\{Ni(dien)]\{Au(CN)_4\}\}_2(\mu\text{-ox})]$ (Figure 3) at the experimental geometry in an idealized $C_{2h}$ symmetry, as models for compounds **1**−**3**, respectively.

The inclusion of relativistic effects and correlation is essential in theoretical calculations of gold complexes to reproduce experimental geometries and propertes.[21] Although the MP2 level of theory predicts geometries of gold complexes in good agreement

(13) (a) Deeming, A. J.; Proud, G. P.; Dawes H. M.; Hursthouse, M. B. *Polyhedron* **1988**, *7*, 651. (b) Yung, W.-F.; Wong, W.-T.; Zuo, J.-L.; Lau, T.-C. *J. Chem. Soc., Dalton Trans.* **2000**, 629.
(14) Smith, J. M.; Jones, L. H.; Kressin, I. K.; Penneman, R. A. *Inorg. Chem.* **1965**, *4*, 369.
(15) Jones, L. H.; Smith, J. M. *J. Chem. Phys.* **1964**, *41*, 2507.
(16) Walker, N.; Stuart, D. *Acta Crystallogr.* **1983**, *A39*, 158.
(17) *International Tables for Crystallography*; Kluwer: Dordrecht, The Netherlands, 1996.
(18) Beurskens, P. T.; Beurskens, G.; Bosman, W. P.; de Gelder, R.; Garcia-Granda, S.; Gould, R. O.; Israel R.; Smits, J. M. M. *DIRDIF96 program system*; Crystallography Laboratory, University of Nijmegen: Nijmegen, The Netherlands, 1996.
(19) Sheldrick, G. M. *SHELX97- Programs for Crystal Structure Analysis (Release 97−2)*; Institüt für Anorganische Chemie der Universität, Tammanstrasse: Göttingen, Germany, 1998.
(20) Farrugia, L. J. *J. Appl. Crystallogr.* **1999**, *32*, 837.

**Table 1.** Crystallographic Data Collection and Structure Determination[a]

| | compd **1** | compd **2** | compd **3** |
|---|---|---|---|
| formula | $C_{10}H_{30}Br_2N_6Ni_2O_6$ | $C_{14}H_{26}Au_2N_{10}Ni_2O_4$ | $C_{14}H_{26}AuF_6N_{10}Ni_2O_4P$ |
| fw | 607.58 | 909.77 | 857.77 |
| space group | $P2_1/c$ (No. 14) | $C2/m$ (No. 12) | $P\bar{1}$ (No. 2) |
| $a$ (Å) | 10.718(2) | 10.5353(8) | 7.1213(6) |
| $b$ (Å) | 7.303(2) | 10.3862(14) | 7.1781(8) |
| $c$ (Å) | 13.296(3) | 12.5381(15) | 14.606(1) |
| α (deg) | | | 77.327(8) |
| $\beta$ (deg) | 96.55(2) | 114.532(8) | 76.757(7) |
| $\gamma$ (deg) | | | 76.621(8) |
| $V$ (Å$^3$) | 1033.9(4) | 1248.1(3) | 696.1(2) |
| $\rho$(obsd), g·cm$^{-3}$ | 2.04 | 2.59 | 2.06 |
| $\rho$(calcd), g·cm$^{-3}$ | 1.95 | 2.421 | 2.05 |
| $Z$ | 2 | 2 | 1 |
| $F$(000) | 612 | 852 | 416 |
| $\mu$ (cm$^{-1}$) | 57.23 | 132.43 | 67.32 |
| R1(obsd rflns) | 0.0507 | 0.0347 | 0.0631 |
| wR2(all rflns) | 0.1200 | 0.0867 | 0.1636 |
| obsd data ($I > 2\sigma(I)$) | 1642 | 2612 | 3987 |
| $S$ | 0.919 | 1.01 | 1.06 |

[a] $R1 = \sum||F_o| - |F_c||/\sum|F_o|$; $wR2 = \{\sum[w(F_o^2 - F_c^2)^2]/\sum[w(F_o^2)^2]\}^{1/2}$.

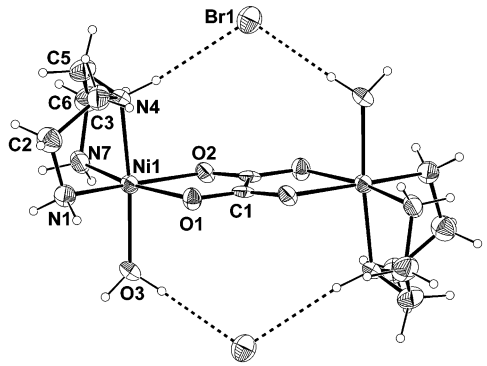


**Figure 1.** ORTEP view of the $[\{Ni(dien)(H_2O)\}_2(\mu\text{-ox})]^{2+}$ cation (**1**) with atom labeling. Probability ellipsoids are 50%.

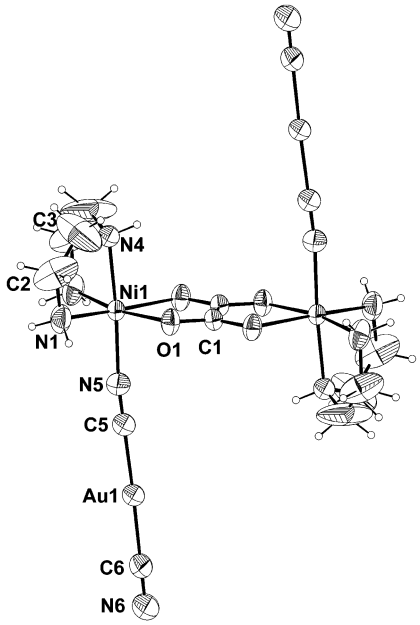


**Figure 2.** ORTEP view of the $[\{Ni(dien)\{Au(CN)_2\}\}_2(\mu\text{-ox})]$ molecule (**2**) with atom labeling. Probability ellipsoids are 50%. This molecule has a crystallographic $C_{2h}$ symmetry.

with experiment,[21b] it is computationally too demanding for systems as large as models **1**−**3**. Hence, density functional theory (B3PW91[22] level of theory), which has been shown to be reliable for studies

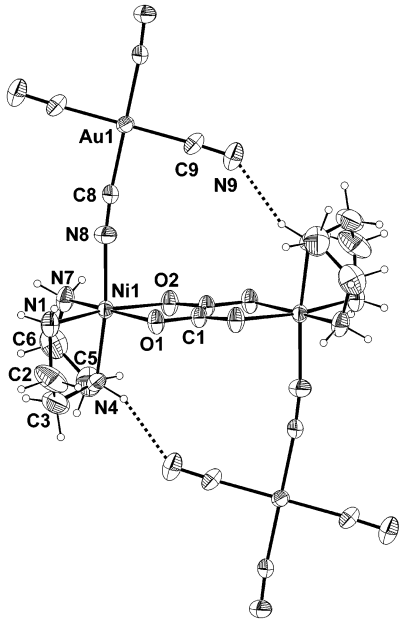


**Figure 3.** ORTEP view of the $[\{Ni(dien)\}_2(\mu\text{-ox})\{(\mu\text{-}Au(CN)_4)\}_2]$ moiety (**3**) with atom labeling. Probability ellipsoids are 50%. In this structure there are crystallographic inversion centers in the middle of the oxalate C−C bonds and in gold positions.

of open-shell Ni(II) coordination compounds,[23] has been used. To incorporate the mass-velocity and Darwin relativistic terms, the Los Alamos effective core potential combined with a DZ basis (LANL2DZ)[24] was chosen for the transition metals, as a compro-

(21) (a) Schwerdtfeger, P.; Boyd, P. D. W.; Burrell, A. K.; Robinson, W. T.; Taylor, M. J. *Inorg. Chem.* **1990**, *29*, 3593. (b) Veldkamp, A.; Frenking, G. *Organometallics* **1993**, *12*, 4613. (c) Rawashdeh-Omary, M. A.; Omary, M. A.; Patterson, H. H.; Fackler, J. P., Jr. *J. Am. Chem. Soc.* **2001**, *123*, 11237.

(22) (a) Becke, A. D. *J. Chem. Phys.* **1993**, *98*, 5648. (b) Burke, K.; Perdew, J. P.; Wang, Y. In *Electronic Density Functional Theory: Recent Progress and New Directions*; Dobson, J. F., Vignale, G., Das, M. P., Eds.; Plenum: New York, 1998. (b) Perdew, J. P. In *Electronic Structure of Solids '91*; Ziesche, P., Eschrig, H., Eds.; Akademie Verlag: Berlin, 1991. (c) Perdew, J. P.; Wang, Y. *Phys. Rev.* **1992**, *B45*, 13244. (d). Perdew, J. P.; Chevary, J. A.; Vosko, S. H.; Jackson, K. A.; Pederson, M. R.; Singh, D. J.; Fiolhais, C. *Phys. Rev.* **1992**, *B46*, 6671. (e) Perdew, J. P.; Chevary, J. A.; Vosko, S. H.; Jackson, K. A.; Pederson, M. R.; Singh, D. J.; Fiolhais, C. *Phys. Rev.* **1993**, *B48*, 4978. (f) Perdew, J. P.; Burke, K.; Wang, Y. *Phys. Rev.* **1996**, *B54*, 16533.

mise between accuracy and the computational power available. For the remaining atoms, the D95V basis[25] was used.

Test calculations for $[Au(CN)_2]^-$ with the above-mentioned theoretical level and basis sets show good agreement between the calculated geometries and properties of the electron density and those predicted using the MP2 level of theory (see Supporting Information).

Single point energy calculations at the experimental geometry for the three models of compounds **1**−**3** and geometry optimizations for the models of compounds **2** and **3** in an idealized $C_{2h}$ symmetry, starting from experimental values, were performed, all of them for open-shell quintets (total $S = 2$). The same theoretical level and basis sets were used to perform geometry optimizations and calculate the electron density in the cyanogold complexes $[Au(CN)_2]^-$ and $[Au(CN)_4]^-$.

All calculations were performed using the Gaussian 98W suite of programs.[26] The electron density was analyzed using Bader's theory of atoms in molecules (AIM),[27] which is a topological analysis of the charge density. A bond path is defined as a line in space of highest charge density $\rho(\mathbf{r})$ linking two nuclei, and its presence provides a universal indicator of bonding between atoms.[28] The point where the charge density reaches a minimal value along this line is termed a bond critical point (BCP), in which the gradient of the density vanishes, $\nabla\rho(\mathbf{r}) = 0$. The nature of the interaction between two atoms linked by a bond path is provided by the density at the bond CP, $\rho(\mathbf{r}_c)$, and its Laplacian, $\nabla^2\rho(\mathbf{r}_c)$. Weak interactions, such as hydrogen bonds, have low $\rho(\mathbf{r}_c)$ and positive values of $\nabla^2\rho(\mathbf{r}_c)$, which indicate a local depletion of charge at the BCP, showing the closed-shell nature of the interaction.

The location and properties of the critical points of the electron density were analyzed with AIM2000[29] and MORPHY,[30] and integrations over the atomic basins were done with PROAIM.[31]

## Results and Discussion

**Synthesis and Spectroscopic Characterization.** In the synthesis of the three compounds, the binuclear complex $[\{Ni(dien)(H_2O)\}_2(\mu\text{-ox})]^{2+}$ was used as a precursor due to the lability of the water molecules which may be substituted by a number of ligands, as can be seen in Scheme 1. The preparation of the compounds was performed as follows: The potassium salt of the corresponding cyanogold complex dissolved in a small amount of water was added to a hot aqueous solution of the precursor binuclear complex. Substitution of the water molecule takes place when dicyanoaurate(I) and tetracyanoaurate(III) complexes are used. Surprisingly, in the case of the bromocyanogold complex, a substitution of hexafluorophosphate by bromide, formed from the dissociation of $[AuBr_2(CN)_2]^-$, takes place, instead of the expected water replacement.

**Table 2.** Theoretical and Experimental $\nu$(CN)[a] IR Band ($cm^{-1}$) for $[M(CN)_n]^{x-}$ Groups

| compd | theoretical[b] | exptl[c] |
|---|---|---|
| $[Au(CN)_2]^-$ | 2158.9 (67.5) | 2147 (477) |
| $[Au(CN)_4]^-$ | 2213.8 (0.34) | 2189 (34) |
| $[Ni(CN)_4]^{2-}$ | 2123.8 (115.5) | 2124 (870) |
| $[Pd(CN)_4]^{2-}$ | 2128.9 (113.9) | 2136 (855) |
| $[Pt(CN)_4]^{2-}$ | 2128.4 (195.2) | 2134 (1265) |

[a] $\Sigma_u$ mode for $[Au(CN)_2]^-$; $E_u$ mode for the rest. [b] Intensity in parentheses ($km\cdot mol^{-1}$). [c] Potassium salts, $\epsilon_{max}$ in parentheses ($M^{-1}\cdot cm^{-1}$) (Memering, M. V.; Jones, L. H.; Bailar, J. C. *Inorg. Chem.* **1973**, *12*, 2793).

Regarding the vibrational behavior of the compounds containing cyanide ligands, it is interesting to underline the extreme weakness of the bands corresponding to CN bond stretching vibrations in compound **3** when compared to those of compound **2**. Frequency calculations using Gaussian 98 for $[M(CN)_n]^{x-}$ groups show good agreement with the experimental data (Table 2). As can be seen in this table, the weakness of CN bond stretching vibrations is also present in the isolated potassium salt of $[Au(CN)_4]^-$.

**Description of the Structures.** The main structural feature of all compounds is the presence of the dinuclear $[\{Ni(dien)(H_2O)\}_2(\mu\text{-ox})]^{2+}$ building block. The oxalate ligand is bonded in a bis(bidentate) fashion to the nickel atoms, and the diethylenetriamine is facially coordinated. The coordination geometry around each nickel ion is $NiN_{6-x}O_x$ distorted octahedral, $x = 3$ for compound **1** and $x = 2$ for compounds **2** and **3**. Thus, the sixth position of coordination is occupied by a water molecule in compound **1** and by a cyanide nitrogen atom in compounds **2** and **3** (Figures 1−3). The Ni−oxalato−Ni fragment adopts in compounds **1** and **3** a chair conformation with a dihedral angle between equatorial and oxalate planes of 5.4(3) and 2.1(4)°, respectively, while in compound **2** this fragment is almost planar [0.9(3)°]. The nickel ions are displaced toward the dien N4 atom by 0.094(6) Å in compound **1** and in compounds **2** and **3** toward the CN nitrogen atom by 0.123(6) and 0.129(9) Å, respectively. Selected bond dimensions for compounds **1**−**3** are listed in Table 3.

**Packing of $[\{Ni(dien)(H_2O)\}_2(\mu\text{-ox})]Br_2$ (1).** The crystal structure of compound **1** projected onto the plane (0 1 0) is shown in Figure 4a. As can be seen, the whole structure has a pronounced two-dimensional arrangement. Inside the layers each dinuclear cation is connected to its neighbors through hydrogen bonds of types N−H···$O_w$, N−H···O, and $O_w$−H···O (Figure 4b). Bromide anions are placed above


(23) (a) Rodríguez, V.; Gutiérrez-Zorrilla, J. M.; Vitoria, P.; Luque, A.; Román, P.; Martínez-Ripoll, M. *Inorg. Chim. Acta* **1999**, *290*, 57. (b) Muga, I.; Gutiérrez-Zorrilla, J. M.; Vitoria, P.; Luque, A.; Insausti, M.; Román, P.; Lloret, F. *Eur. J. Inorg. Chem.* **2000**, 2541.

(24) (a) Hay, P. J.; Wadt, W. R. *J. Chem. Phys.* **1985**, *82*, 270. (b) Wadt W. R.; Hay, P. J. *J. Chem. Phys.* **1985**, *82*, 284.. (c) Hay, P. J.; Wadt, W. R. *J. Chem. Phys.* **1985**, *82*, 299.

(25) Dunning, T. H., Jr.; Hay, P. J. In *Modern Theoretical Chemistry;* Schaefer, H. F., III, Ed.; Plenum: New York, 1976.

(26) Frisch, M. J.; Trucks, G. W.; Schlegel, H. B.; Scuseria, G. E.; Robb, M. A.; Cheeseman, J. R.; Zakrzewski, V. G.; Montgomery, J. A.; Stratmann, R. E.;. Burant, J. C.; Dapprich, S.; Millam, J. M.; Daniels, A. D.; Kudin, K. N.; Strain, M. C.; Farkas, O.; Tomasi, J.; Barone, V.; Cossi, M.;. Cammi, R; Mennucci, B.; Pomelli, C.; Adamo, C.; Clifford, S.; Ochterski, J.; Petersson, G. A.; Ayala, P. Y.; Cui, Q.; Morokuma, K.; Malick, D. K.; Rabuck, A. D.; Raghavachari, K.; Foresman, J. B.; Cioslowski, J.; Ortiz, J. V.; Stefanov, B. B.; Liu, G.; Liashenko, A.; Piskorz, P.; Komaromi, I.; Gomperts, R.; Martin, R. L.; Fox, D. J.; Keith, T.; Al-Laham, M. A.; Peng, C. Y.; Nanayakkara, A.; Gonzalez, C.; Challacombe, M.; Gill, P. M. W.; Johnson, B. G.; Chen, W.; Wong, M. W.; Andres, J. L.; Head-Gordon, M.; Replogle E. S.; Pople, J. A. *Gaussian 98W (Revision A.7)*; Gaussian, Inc.: Pittsburgh, PA, 1998.

(27) Bader, R. F. W. *Atoms in molecules−A quantum theory*; International Series of Monographs on Chemistry, No. 22; Oxford University Press: Oxford, U.K., 1990.

(28) Bader, R. F. W. *J. Phys. Chem. A* **1998**, *102*, 7314.

(29) Biegler-König, F.; Schönbohm, J.; Bayles, D. *J. Comput. Chem.* **2001**, *22*, 545.

(30) Popelier, P. L. A. *Comput. Phys. Commun.* **1996**, *93*, 212.

(31) Biegler-König, F.; Bader, R. F. W.; Tang, T.-H. *J. Comput. Chem.* **1982**, *13*, 317.

**Table 3.** Selected Bond Distances and Angles for Compounds **1**−**3**[a]

| | compd **1** | compd **2** | | compd **3** | |
|---|---|---|---|---|---|
| | | Ni Coordination Sphere | | | |
| Ni1−O1 | 2.099(3) | 2.104(2) | *2.076* | 2.080(5) | *2.083* |
| Ni1−O2 | 2.106(3) | | | 2.087(5) | |
| Ni1−N1 | 2.076(4) | 2.083(4) | *2.077* | 2.067(6) | *2.087* |
| Ni1−N4 | 2.082(5) | 2.075(5) | *2.087* | 2.089(8) | *2.095* |
| Ni1−N7 | 2.059(4) | | | 2.086(6) | |
| Ni1−X[b] | 2.080(4) | 2.058(5) | *2.082* | 2.096(8) | *2.111* |
| O1−Ni1−O2[c] | 79.5(1) | 79.3(1) | *81.5* | 80.3(2) | *80.8* |
| O1−Ni1−N1 | 90.0(2) | 90.1(1) | *85.9* | 90.0(2) | *85.9* |
| O1−Ni1−N4 | 92.6(2) | 92.7(1) | *92.5* | 96.0(3) | *97.7* |
| O1−Ni1−N7[d] | 169.2(2) | 168.4(1) | *166.9* | 170.0(2) | *166.7* |
| O1−Ni1−X | 91.4(2) | 90.3(1) | *90.6* | 91.6(2) | *91.3* |
| O2−Ni1−N1 | 169.3(2) | | | 169.0(2) | |
| O2−Ni1−N4 | 94.9(2) | | | 92.9(2) | |
| O2−Ni1−N7 | 90.5(2) | | | 90.1(2) | |
| O2−Ni1−X | 88.5(2) | | | 91.1(2) | |
| N1−Ni1−N4 | 83.5(2) | 82.9(1) | *84.7* | 82.9(3) | *84.4* |
| N1−Ni1−N7 | 99.9(2) | 99.9(2) | *106.5* | 99.3(2) | *107.5* |
| N1−Ni1−X | 93.8(2) | 94.6(1) | *92.9* | 94.4(3) | *88.6* |
| N4−Ni1−N7 | 84.4(2) | | | 81.7(3) | |
| N4−Ni1−X | 175.2(2) | 176.2(2) | *175.9* | 171.9(3) | *168.2* |
| N7−Ni1−X | 92.2(2) | | | 91.3(3) | |
| Ni−N−C | | 174.2(5) | *138.6* | 172.4(7) | *168.8* |
| | | $[Au(CN)_2]^-$ Group | | | |
| Au1−C5 | | 1.979(5) | *1.990* | | |
| Au1−C6 | | 1.981(6) | *1.989* | | |
| C5−N5 | | 1.139(7) | *1.188* | | |
| C6−N6 | | 1.145(9) | *1.189* | | |
| Au1−C5−N5 | | 180.0(5) | *170.3* | | |
| Au1−C6−N6 | | 179.6(4) | *173.8* | | |
| C5−Au1−C6 | | 178.5(3) | *173.3* | | |
| | | $[Au(CN)_4]^-$ Group | | | |
| Au1−C8 | | | | 1.993(8) | *2.022/1.995* |
| Au1−C9 | | | | 1.982(7) | *2.019/2.003* |
| C8−N8 | | | | 1.138(11) | *1.178/1.182* |
| C9−N9 | | | | 1.150(10) | *1.178/1.183* |
| Au1−C8−N8 | | | | 175.0(7) | *174.2* |
| Au1−C9−N9 | | | | 177.7(7) | *171.9/177.7* |
| C8−Au1−C9 | | | | 87.4(3) | *91.2* |
| C8−Au1−C9 | | | | 92.6(3) | *86.2* |
| C8−Au1−C8 | | | | 180.0 | *178.3* |
| C9−Au1−C9 | | | | 180.0 | *177.5* |

[a] DFT data for compounds **2** and **3** are shown in italics. [b] X = O3 for compd **1**, N5 for compd **2**, and N8 for compd **3**. [c] For compd **2** O1′ (*x*, 1 − *y*, *z*). [d] For compd **2** N1′ (*x*, 1 − *y*, *z*).

and below each dinuclear complex, forming two hydrogen bonds that connect N4 and the coordinated water molecule. They also contribute to the packing connecting the four nearest $[\{Ni(dien)(H_2O)\}_2(\mu\text{-ox})]^{2+}$ cations via hydrogen bonds involving the water molecules and the three dien nitrogen atoms. A remarkable aspect of the salts containing this binuclear cation complex is the different degree of hydration, which becomes higher as the anion becomes larger. All salts present a 2D arrangement in which the layers are connected by van der Waals forces, but the hydrogen bond network inside these layers are strongly dependent on the anion and the number of water molecules. Moreover, there is a correlation between the volume of anion[32] and the intermolecular Ni···Ni distances (Figure 5).

**$[\{Ni(dien)(Au(CN)_2)\}_2(\mu\text{-ox})]$ (2).** The crystal structure of compound **2** presents a bidimensional arrangement parallel to (0 0 1) plane, where each neutral complex is connected

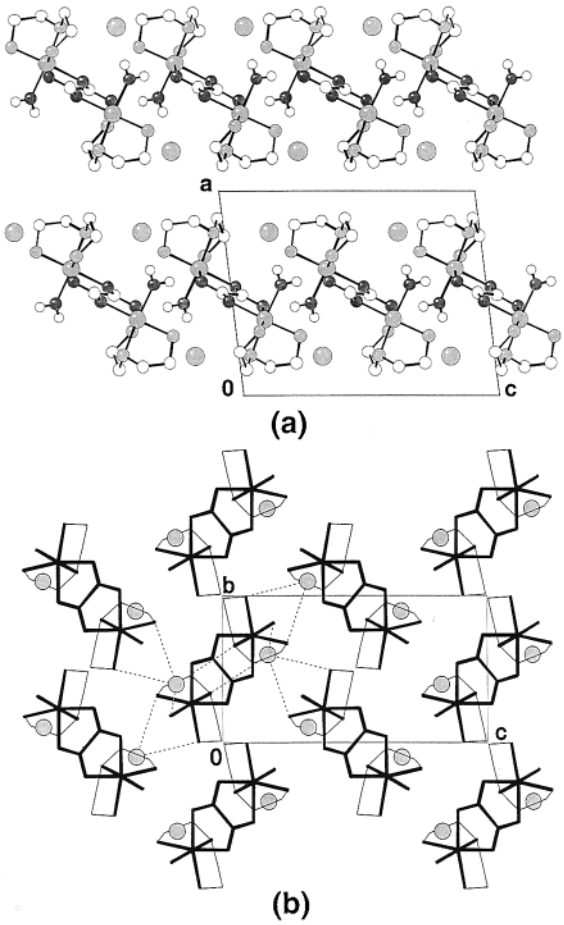


**Figure 4.** Compound **1**: (a) Packing diagram viewed down the *b* axis; (b) arrangement in a shell showing the hydrogen bonding network around a $[\{Ni(dien)(H_2O)\}_2(\mu\text{-ox})]^{2+}$ group. H atoms are omitted for clarity.

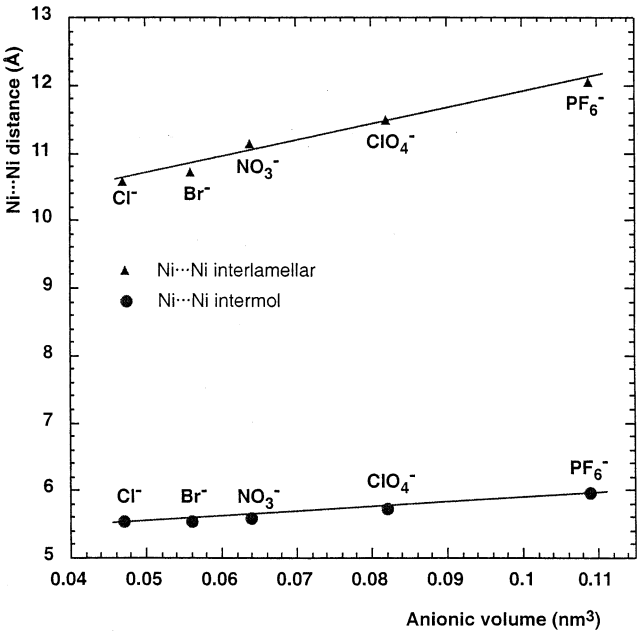


**Figure 5.** Correlation diagram between Ni···Ni distances (Å) and the counteranion volume ($nm^3$) for $[\{Ni(dien)(H_2O)\}_2(\mu\text{-ox})]X_2{\cdot}nH_2O$ compounds.

through eight hydrogen bonds of type N1−H1···O1 (Figure 6a), The $[Au(CN)_2]^-$ group acts as a terminal ligand replacing

(32) Jenkins, H. D. B.; Roobottom, H. K.; Passmore, J.; Glasser, L. *Inorg Chem*. **1999**, *38*, 3609.

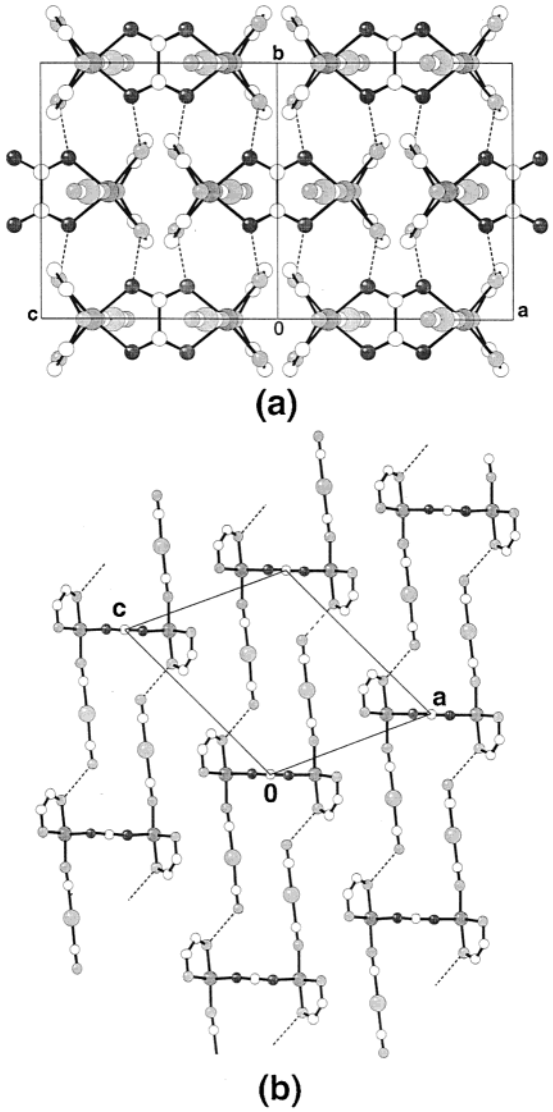


**Figure 6.** Compound **2**: (a) Arrangement of $[\{Ni(dien)\{Au(CN)_2\}\}_2(\mu\text{-ox})]$ molecules in a shell showing the hydrogen bonding network (all hydrogen bonds are of type N1−H1···O1); (b) view along the *b* axis showing the molecules hydrogen bonded along the [1 0 1] direction.

the water molecule with a linear coordination, Ni−N8−C8 angle of 176.3°. This value is larger than the reported value for another known compound, $[Cu(cyclem)\{Au(CN)_2\}][Au(CN)_2]$,[13b] with the $[Au(CN)_2]^-$ group acting as a terminal ligand, which is 157°. This group plays an important role in the stability of the structure. Each terminal noncoordinated CN group is buried into the nearest layer in order to form the hydrogen bond N4−H4···N6, which keeps connected all layers along the [1 0 1] direction (Figure 6b), and gives to the structure a three-dimensional character which contrasts with the pronounced layered structure observed in other compounds which contain the $[\{Ni(dien)\}_2(\mu\text{-ox})]^{2+}$ building block.

**$[\{Ni(dien)\}_2(\mu\text{-ox})\{(\mu\text{-}Au(CN)_4)\}](PF_6)$ (3).** The structure of compound **3** is comprised of dinuclear $[\{Ni(dien)\}_2(\mu\text{-ox})]^{2+}$ blocks bridged by $[Au(CN)_4]^-$ anions to form chains parallel to the [1 −1 0] direction, and noncoordinated $PF_6^-$ anions (Figure 7a). The whole structure has a pronounced two-dimensional character and can be viewed as a succession

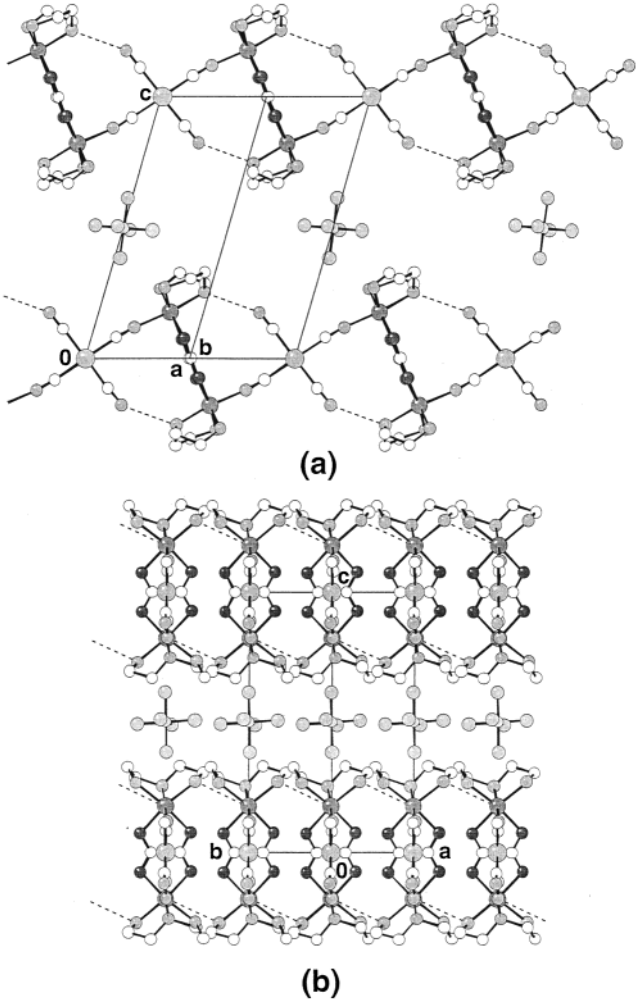


**Figure 7.** Compound **3**: (a) View of chains $[\{Ni(dien)\}_2(\mu\text{-ox})]\{\mu\text{-}Au(CN)_4\}]_n^{n+}$ showing both types of connections played by the $[Au(CN)_4]^-$ anion; (b) arrangement of the chains showing the layer packing.

along the *c* axis of layers of nickel−gold complexes separated by layers of $PF_6^-$ anions (Figure 7b). Each layer of metal complexes is built up by chains $[\{Ni(dien)\}_2(\mu\text{-ox})]\{\mu\text{-}Au(CN)_4\}]_n^{n+}$, where each binuclear group is connected to the nearest four groups of adjacent chains through hydrogen bonds of the type N1−H1···N9. Although compounds with tetracyanometalates, mainly of group 8 metals, acting as bridging ligands are known,[33] compound **3** is the first example in which the tetracyanoaurate complex appears as a bridging ligand between $[\{Ni(dien)\}_2(\mu\text{-ox})]^{2+}$ units. Each building block is connected in two fashions to both adjacent gold atoms, through the covalent bond Au−C8−N8−Ni and the hydrogen bond Ni−N4−H4···N9−C9−Au.

**Magnetic Properties.** The thermal dependence of the molar magnetic susceptibility, $\chi_M$, of compounds **1**−**3** (Figure 8) is characteristic of an antiferromagnetic interaction between the two single-ion triplet states: the value of $\chi_M$ at room temperature is in the range expected for two $S = 1$

(33) (a) Yuge, H.; Iwamoto T. *J. Chem. Soc., Dalton Trans.* **1994**, 1237. (b) Cernak, J.; Chomic, J.; Domiano, P.; Ori, O.; Andreetti G. D. *Acta Crystallogr.* **1990**, *C46*, 2103. (c) Cernak, J.; Chomic, J.; Baloghova, D.; Dunaj-Jurco M. *Acta Crystallogr.* **1988**, *C44*, 1902. (d) Zhan, S.; Guo, D.; Zhang, X.; Du, C.; Zhu, Y.; Yang R. *Inorg. Chim. Acta* **2000**, *298*, 57.

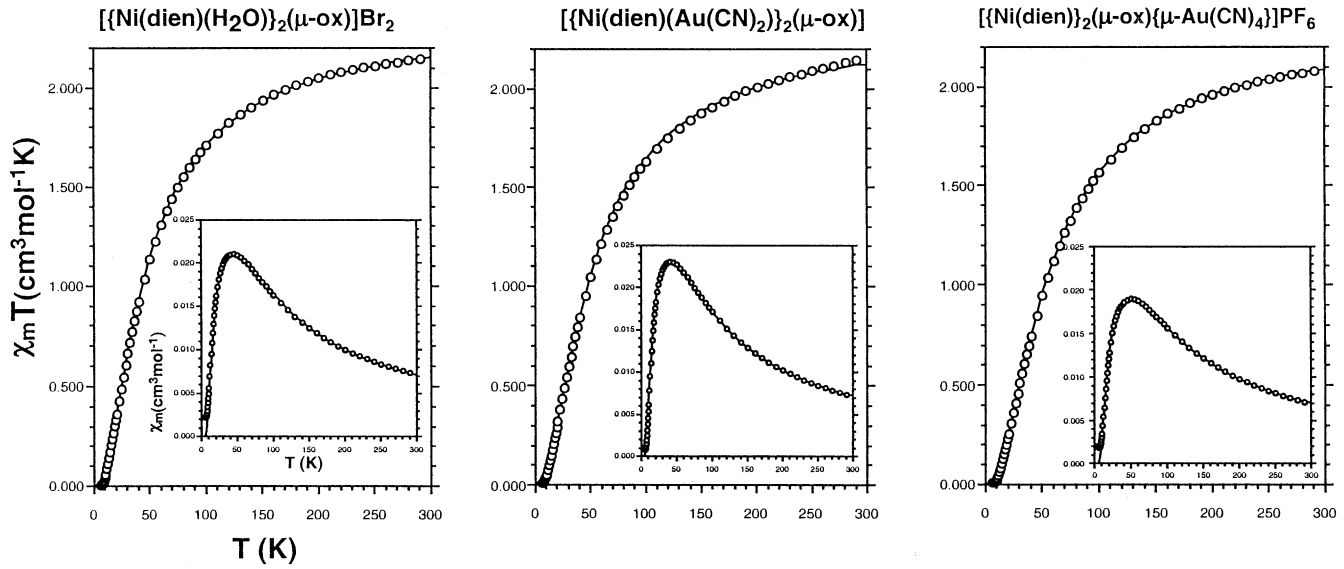


**Figure 8.** Magnetic behavior for compounds **1**−**3**.

**Table 4.** Selected Magnetostructural Parameters [Å, deg] for Compounds Containing the $[\{Ni(dien)\}_2(\mu\text{-ox})]^{2+}$ Building Block[a]

$NiN_3O_3$ Environment

| compd | *J* | *g* | Ni−$O_{ox}$ | Ni−$N_{eq}$ | Ni−$N_{ap}$ | Ni−$O_{ap}$ | O−Ni−O | Ni···Ni | *h*(Ni) | ref |
|---|---|---|---|---|---|---|---|---|---|---|
| $[\{Ni(dien)(H_2O)\}_2(\mu\text{-ox})]Cl_2$ | 28. 8 | 2.1 0 | 2.125/ 2.112 | 2.123/ 2.082 | 2.11 0 | 2.10 5 | 79.3 | 5.48 8 | 0.070 | 3f |
| $[\{Ni(dien)(H_2O)\}_2(\mu\text{-ox})]Br_2$ | 28. 1 | 2.1 8 | 2.106/ 2.099 | 2.059/ 2.076 | 2.08 2 | 2.08 0 | 79.5 | 5.46 9 | 0.094 | **1** |
| $[\{Ni(dien)(H_2O)\}_2(\mu\text{-ox})](NO_3)_2$ | 27. 2 | 2.2 0 | 2.112/ 2.108 | 2.082/ 2.064 | 2.07 6 | 2.09 3 | 78.9 | 5.48 7 | 0.062 | 12f |
| $[\{Ni(dien)(H_2O)\}_2(\mu\text{-ox})](PF_6)_2\cdot 2H_2O$ | 28. 7 | 2.1 8 | 2.111/ 2.101 | 2.069/ 2.071 | 2.08 0 | 2.10 4 | 79.4 | 5.45 8 | 0.067 | 12g |

$NiN_4O_2$ Environment

| compd | *J* | *g* | Ni−$O_{ox}$ | Ni−$N_{eq}$ | Ni−$N_{ap}$ | Ni−$N'_{ap}$ | O−Ni−O | Ni···Ni | *h*(Ni) | ref |
|---|---|---|---|---|---|---|---|---|---|---|
| $[\{Ni(dien)(N_3)\}_2(\mu\text{-ox})]$ | 31. 4 | 2.2 5 | 2.081 | 2.079 | 2.10 6 | 2.15 4 | 80.8 | 5.39 7 | 0.021 | 12c |
| $[\{Ni(dien)(NCO)\}_2(\mu\text{-ox})\ ]$ | 28. 5 | 2.1 4 | 2.108 | 2.082 | 2.12 2 | 2.09 1 | 79.2 | 5.49 1 | 0.198 | 12c |
| $[\{Ni(dien)(NCS)\}_2(\mu\text{-ox})]$ | 33. 0 | 2.0 8 | | | | | | | | 12c |
| $[\{Ni(dien)(Au(CN)_2)\}_2(\mu\text{-ox})]$ | 30. 7 | 2.1 7 | 2.104 | 2.083 | 2.07 5 | | 79.3 | 5.39 7 | 0.021 | **2** |
| $[\{Ni(dien)\}_2(\mu\text{-ox})(\mu\text{-}Au(CN)_4)]PF_6$ | 33. 8 | 2.1 7 | 2.080/ 2.087 | 2.067/ 2.089 | 2.08 9 | 2.09 6 | 80.3 | 5.41 9 | 0.129 | **3** |

[a] Abbreviations used: dien = diethylenetriamine; *J* in $cm^{-1}$; Ni−$O_{ox}$ = distance Ni−O(oxalato); Ni−$N_{eq}$ = distance Ni−N(dien−equatorial); Ni−$N_{ap}$ = distance Ni−N(dien−apical); Ni−$O_{ap}$ = distance Ni−O(water); Ni−$N'_{ap}$ = distance Ni−N(apical); *d*(Ni···Ni) = nickel−nickel separation across the oxalato ligand; O−Ni−O = bite angle; *h*(Ni) = metal height from the oxalato mean plane.

states ($\mu_{eff}$ ca. 4 $\mu_B$ for **1**−**3**). The susceptibility curve for these complexes increases when the compound is cooled until a maximum is reached ($T_{max}$ = 40, 45, and 50 K, for **1**−**3**, respectively) and finally decreases very quickly. The intradimer exchange interaction, *J*, in dinuclear nickel(II) complexes can be treated with the isotropic spin Hamiltonian $H = -JS_AS_B$.[34] The molar magnetic susceptibility for a nickel(II) dimer (local spins $S_A = S_B = 1$) may be expressed by

$$\chi_M = \frac{2N\beta^2g^2}{kT}\frac{\exp(J/kT) + 5\exp(3J/kT)}{1 + 3\exp(J/kT) + 5\exp(3J/kT)} \qquad (1)$$

where *N* is Avogadro's number; $\beta$, Bohr magneton; *k*, Boltzmann's constant; *g*, gyromagnetic ratio; and *T*, absolute temperature. Although, nickel(II) in an axial symmetry can have a large zero-field splitting, *D*, the magnetic behavior of nickel(II) dimers closely follows eq 1 when a relatively strong antiferromagnetic interaction is operative,[35] which makes the consideration of *D* unnecessary. This is the case for complexes **1**−**3** for which least-squares analysis of the experimental data using eq 1 leads to $J = -28.1$ $cm^{-1}$, $g = 2.18$, and $R = 3.2 \times 10^{-8}$ for **1**; $J = -30.7$ $cm^{-1}$, $g = 2.17$, and $R = 7.8 \times 10^{-7}$ for **2**; $J = -33.8$ $cm^{-1}$, $g = 2.17$, and $R = 3.6 \times 10^{-7}$ for **3**. *R* is the agreement factor defined as $R = [\Sigma(\chi_M^{obs} - \chi_M^{calc})^2/(n - k)]^{1/2}$, where *n* is the number of points and *k* is the number of variables. Previously reported *J* values for compounds containing the $[\{Ni(dien)(H_2O)\}_2(\mu\text{-ox})]^{2+}$ building block are close to those of compounds **1**−**3**. This information is summarized in Table 4 for dinuclear $Ni^{II}$-oxalate systems in $NiO_2N_4$ and $NiO_3N_4$ environments. It is well-known that structural distortions (distance Ni−$O_{ox}$, bite angle O−Ni−O, deviation from the planarity of the nickel atom with respect to the mean plane of the oxalate bridging ligand) can play a key role in the fine-tuning of exchange coupling. Single-point energy cal-

(34) Castro, I.; Calatayud, M. L.; Sletten, J.; Lloret, F.; Julve, M. *J. Chem. Soc., Dalton Trans.* **1996**, 811.

(35) De Munno, G.; Julve, M.: Lloret, F.; Derory, A. *J. Chem. Soc., Dalton Trans.* **1993**, 1179.

**Table 5.** Geometries and Topological Properties[a] of the Electron Density at the Bond Critical Point of Intramolecular N−H···X Hydrogen Bonds[a]

| N−H···X | $d$(N···X) (Å) | $d$(H···X) (Å) | α(NHX) (deg) | $\rho \times 100$ | $\nabla^2\rho \times 100$ | $\lambda_3 \times 100$ | $\lambda_3/\bar{\lambda}_{1,2}$ | $\epsilon$ |
|---|---|---|---|---|---|---|---|---|
| X = Au model of **2** | 3.792 | 2.798 | 163.7 | 0.95 | 3.1 | 4.4 | 6.4 | 0.43 |
| X = N model of **3** | 2.851 | 1.837 | 165.5 | 3.7 | 12.1 | 23.6 | 4.1 | 0.018 |
| compd **3** | 3.136 | 2.3 | 152.3 | | | | | |

[a] If not otherwise stated, all quantities are in atomic units. $\rho$, electron density; $\nabla^2\rho$, laplacian of the electron density; $\lambda_3$, curvature of the electron density along the bond path; $\bar{\lambda}_{1,2}$, average of the two perpendicular curvatures $\lambda_1$ and $\lambda_2$; $\epsilon$, ellipticity $[(\lambda_2/\lambda_1) - 1]$.

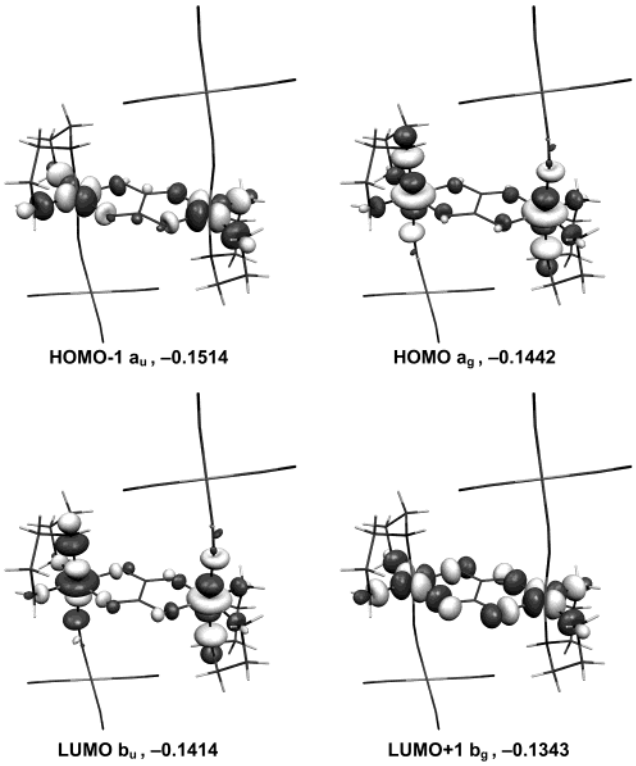


**Figure 9.** Magnetic orbitals for compound **3** (symmetry, energy).

culations for the three compounds show a relation between the $\Delta E$ (the energy splitting for molecular orbitals with a $d_{x^2-y^2}$ or $d_{z^2}$ character), the $J$ values and the electronegativity of the apical atom. Thus, the $\Delta E(d_{x^2-y^2})$ values are 0.0159 au for **1**, 0.01695 au for **2**, and 0.01708 au for **3**, while the $d_{z^2}$ are practically degenerated. It can be observed that an increase in the number of nitrogen donor atoms in the coordination sphere of Ni atoms results in an increase in the $\Delta E$ values because the less electronegative terminal atoms interact in a more efficient way with the metal d orbitals due to a better energy match.[3f]

A graphical representation of the four DFT magnetic orbitals of compound **3** is given in Figure 9, with those for compounds **1** and **2** being very similar. As expected for the case of octahedral nickel(II) centers, the unpaired electrons are mainly located in the $d_{z^2}$ and $d_{x^2-y^2}$ orbitals. In contrast to other pseudohalide derivatives,[12c] there is no contribution of the axial ligand $\pi$ orbitals to the $d_{z^2}$ magnetic orbital.

**DFT Calculations: $[Au(CN)_2]^-$ versus $[Au(CN)_4]^-$.** A study of the nickel coordination geometry in compounds **2** and **3** reveals the existence of a noticeable difference in the Ni−NCAu bond distance (Table 3). To explain this fact, DFT calculations were performed for the isolated molecular dimers $[\{Ni(dien)\{Au(CN)_2\}\}_2(\mu\text{-ox})]$ and $[\{Ni(dien)\}\{Au(CN)_4\}\}_2(\mu\text{-ox})]$ in an idealized $C_{2h}$ symmetry, as models for compounds **2** and **3**, respectively. The calculations agree very well with the experimental data in which the Ni−NCAu bond distance is longer for compound **3**. This means that this elongation is not due to the fact that in compound **3** the tetracyanoaurate acts as a bridging ligand and in compound **2** the dicyanoaurate is a terminal ligand. The explanation must reside in the electronic structure of both cyanogold groups. As the oxidation state of gold becomes higher, the strong $\sigma$-donor cyanide ligands have less electron density on the nitrogen atoms to coordinate to the nickel atoms. This is corroborated by AIM calculations of the integrated charge density over the atomic basins for $[Au(CN)_2]^-$ and $[Au(CN)_4]^-$ anions, which show a higher charge over the $[Au(CN)_2]^-$ cyanide groups, −0.65 au, than over $[Au(CN)_4]^-$ cyanides, −0.48 au.

As can be seen in Table 3, the agreement between experimental and calculated values for bond distances and angles is quite good except for the Ni−N≡C bond angle in compound **2**. In the crystal structure the $[Au(CN)_2]^-$ group acts as a terminal ligand with a nearly linear coordination, Ni−N8−C8 angle of 176.3°, so that each terminal noncoordinated CN group forms the hydrogen bond N4−H4···N6, forming a chain of binuclear complexes. On the other hand, in the optimized isolated molecule, where the formation of intermolecular hydrogen bonds is not possible, the dicyanogold ligand bends (Ni−N≡C bond angle = 138.6°) to form an intramolecular hydrogen bond of type N−H···Au (Table 5). The existence of hydrogen bonds where the proton acceptor is a late transition metal in a low oxidation state has been well-established in recent years.[36]

The optimization of compound **3** model leads to an intramolecular hydrogen bond of type N−H···N≡C, which is also present in the crystal structure. The data in Table 5 show that the model hydrogen bond is stronger than the one present in the crystal structure, probably because the tetracyanoaurate(I) group has more freedom to bend toward the NH donor in the model than in compound **3**, where it connects binuclear units to form a chain.

This type of hydrogen bond has been studied through the analysis of the charge density using the theory of atoms in molecules, which has been shown, both in experimental and theoretical studies, to be able to establish the presence of hydrogen bonding through the fulfillment of a set of criteria.[37] In the electron density of the optimized models of compounds

(36) (a) Brammer, L.; Zhao, D.; Ladipo, F. T.; Braddock-Wilking, J. *Acta Crystallogr.* **1995**, *B51*, 632. (b) Braga, D.; Grepioni, F.; Tedesco, E.; Biradha, K.; Desiraju, G. R. *Organometallics* **1997**, *16*, 1846. (c) Martín, A. *J. Chem. Educ.* **1999**, *76*, 578. (d) Calhorda, M. J. *Chem. Commun.* **2000**, 801.

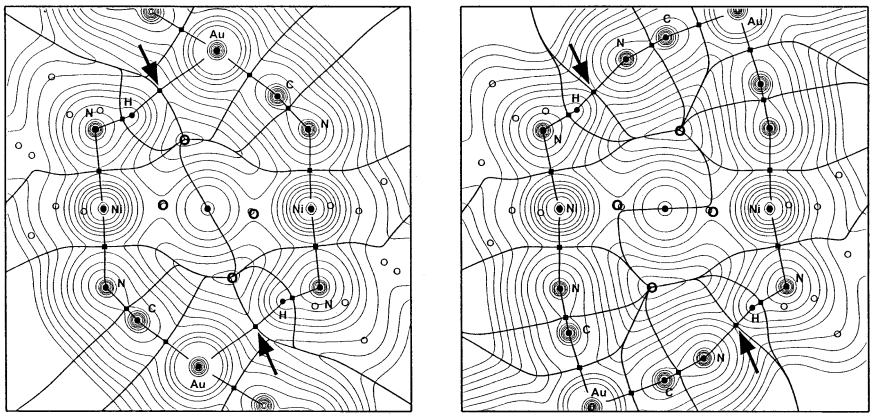


**Figure 10.** Molecular graphs determined by the topology of the electron density in the plane containing the four metallic atoms for optimized structures of compounds **2** and **3**. Positions of the bond and ring CPs are denoted by filled squares and bold open circles, respectively. Arrows point to the hydrogen bond critical points.

**2** and **3**, a bond critical point and its associated bond path is found between the H of the dien-NH group and the corresponding proton acceptor atom, Au in compound **2** and cyanide N in compound **3** (Figure 10).

As can be seen in Table 5, the topological properties for the two kinds of hydrogen bonds indicate that the N−H···N bond is stronger than the N−H···Au bond. This can explain the absence of the N−H···Au intramolecular hydrogen bond in the crystal structure of compound **2**, because the formation of a stronger intermolecular N−H···N bond is favored for both thermodynamic and crystal stability reasons.

## Conclusions

The reaction between cyanogold complexes and the cationic complex $[\{Ni(dien)(H_2O)\}_2(\mu\text{-ox})]^{2+}$ results in a variety of compounds, depending on the nature of the gold complex, ranging from simple anion substitution of the starting material to the water displacement leading to di- or polynuclear compounds.

Compound **3** is the first example in which the tetracyanoaurate acts as a ligand, in this case as a bridging ligand to give a polymeric compound.

It has been shown that DFT calculations are able to reproduce the experimental geometries and properties of gold containing coordination compounds and to establish the presence of hydrogen bonds involving both classical (N) and late transition metal proton acceptors.

**Acknowledgment.** This work was supported by Ministerio de Educación y Cultura (Grant No. PB98/ 0238). We thank the reviewers for their helpful comments and suggestions.

**Supporting Information Available:** Crystallographic data in CIF format for compounds **1**−**3,** bond distances and topological properties of the electron density at the Au−C bond critical points. This material is available free of charge via the Internet at http://pubs.acs.org

IC0203217

(37) Koch, U.; Popelier, P. L. A. *J. Phys. Chem.* **1995**, *99*, 9747.